Moment tensor inversion for Iberia–Maghreb earthquakes 2005–2008

Daniel Stich *, Rosa Martín, Jose Morales

Instituto Andaluz de Geofísica, Universidad de Granada, Spain

A R T I C L E   I N F O

A B S T R A C T

We present and discuss a set of 77 moment tensor solutions for earthquakes in the Iberia–Maghreb region from mid 2005 to the end of 2008, with moment magnitudes ranging from 3.2 to 6.0. Inversion is based upon full, three-component, intermediate period waveforms recorded at regional seismic broadband stations. Following the recent densification of permanent broadband networks and large scale temporary deployments, at present more than 150 stations are recording in Spain, Portugal and Morocco. This unprecedented station density allows analysis of small events from available short-distance recordings, and in general leads to more reliable source estimates due to data redundancies that permit elimination of waveforms affected by noise or complicated propagation effects. The solutions for 2005–2008 constitute an important upgrade of the Iberia–Maghreb moment tensor inventory to 225 solutions to date, enhancing the image of seismotectonics at the compressive N-Algerian margin, in the Betic–Alboran shear zone and at the transpressive SW-Iberian margin, as well as providing valuable constraints on seismic deformation in the western Betics and the Iberian foreland where little information has been previously available. New solutions for the foreland and three recent seismic series in the western Betics show strike-slip and reverse faulting style, contrasting with the dominance of normal faulting in the adjacent areas towards east. In these areas, as well as at the SW-Iberian margin, faulting orientations are heterogeneous, including solutions with opposite kinematics. This indicates control by local stress conditions, and points to fault interaction. Along the N-Algerian margin, a counterclockwise rotation of slip vectors of thrust events from east to west becomes apparent. Several solutions for the area offshore Cape St. Vincent are located at sub-Moho depths between 40 and 60 km, supporting a large brittle layer thickness in the oceanic lithosphere.

© 2009 Elsevier B.V. All rights reserved.

1. Introduction

As Earth science advances towards a more detailed and comprehensive understanding of lithospheric dynamics at regional scale, the completeness and coverage of the individual data sets involved is gaining major importance. Often the apparent homogeneity of some parameter over some area may have been an artifact of a too sparse data sampling, while newly available data may fill the gaps and contribute to a more realistic picture. In this article we report on our recent effort to achieve a better regional coverage for the case of seismic moment tensor estimates in the Iberia–Maghreb area. Seismic source estimates pose an intrinsic problem with respect to full regional coverage, that is, earthquakes exceeding a certain magnitude tend to be concentrated in belts of active deformation. In the Iberia–Maghreb region we observe that seismicity is distributed diffusely in a relative wide belt around the presumed present-day plate contact (e.g. Buforn et al., 1995; Stich et al., 2006), and earthquakes occur as well in the foreland at significant distances from the plate boundary zone. This situation is favorable for our goal, but complications arise

from the typically small magnitudes of earthquakes outside the main seismogenic zones, making moment tensor estimates for the rest of the region more difficult to obtain.

Seismic moment tensors for moderate and large events in the Iberia–Maghreb region (Mw>5) are provided routinely within global initiatives (Global CMT catalogue, Dziewonski and Woodhouse, 1983; USGS-NEIC, Sipkin, 1982). Moment tensor projects at European–Mediterranean scale include the more frequent smaller magnitude events down to Mw ~4 and provide a much larger number of solutions (ETH moment tensor catalogue, Braunmiller et al., 2002; INGV Regional CMT catalogue, Pondrelli et al., 2002). The magnitude threshold is pushed further in Iberia–Maghreb-scale moment tensor projects, including the automated near real-time inversion by the Instituto Geográfico Nacional (IGN, Rueda and Mézcua, 2005) and the processed moment tensor solutions provided by the Instituto Andaluz de Geofísica (IAG, Stich et al., 2003, 2006). These catalogues, as well as individual studies (Cesca et al., 2006) show that regional moment tensor inversion for events as small as Mw 3.3 is possible under favorable conditions, but still earthquakes with magnitude less than 4 are underrepresented, contributing only ~30% of the solutions to the IAG and IGN catalogues. The different magnitude thresholds in global, continental-scale and regional-scale moment tensor catalogues reflect the different scope of these projects, and are related to the density of

* Corresponding author.
E-mail address: daniel@iag.ugr.es (D. Stich).

the seismic recording networks involved. Dense regional station networks record small events at short distances, generally corresponding to better signal-to-noise ratio and less complicated propagation effects, thus creating more favorable conditions for the inversion of small earthquakes around Mw 3.5 (e.g. Braunmiller et al., 2002; Clinton et al., 2006).

In the Iberia–Maghreb region, important efforts have been undertaken towards improving the coverage with broadband seismic stations. This includes the upgrade and densification of permanent networks like those operated by the Spanish IGN, IAG and IGC (Institut Geològic de Catalunya), Portuguese Instituto de Meteorologia (IM) or through the international cooperation of Geofon/ROA/UCM, as well as dense temporary deployments including the east Betic network operated by IAG and the first phase of the regional-scale TopoIberia experiment (Díaz et al., 2009). The average spacing of broadband seismic stations is now around 50 km in the southern and northeastern part of the Iberian Peninsula, and locally only 30 km in areas in SE Spain and Catalonia (Fig. 1). We show how the use of this dense recording network allows inclusion of a larger percentage of small

earthquakes in our moment tensor catalogue, and present our results for the seismicity during the 3.5-year period from mid 2005 to the end of 2008. We refer to previous publications (Stich et al. (2003, 2006), and references therein) for a more detailed description of the inversion methodology (summarized in Section 2) and for a discussion of the seismotectonic framework (summarized in Section 3), and concentrate on the interpretation of the new solutions here, many of which are from sampling areas where earthquake source parameter information was previously scarce, or absent.

2. Moment tensor inversion

The first order seismic moment tensor is a general description of the equivalent body forces for a seismic point source. It contains information on scalar seismic moment (Silver and Jordan, 1982) and moment magnitude Mw (Hanks and Kanamori, 1979), as well as the orientation and mechanism of the source. According to the representation theorem, the moment tensor links the observed seismograms linearly to a set of fundamental Greens functions (e.g. Langston et al.,
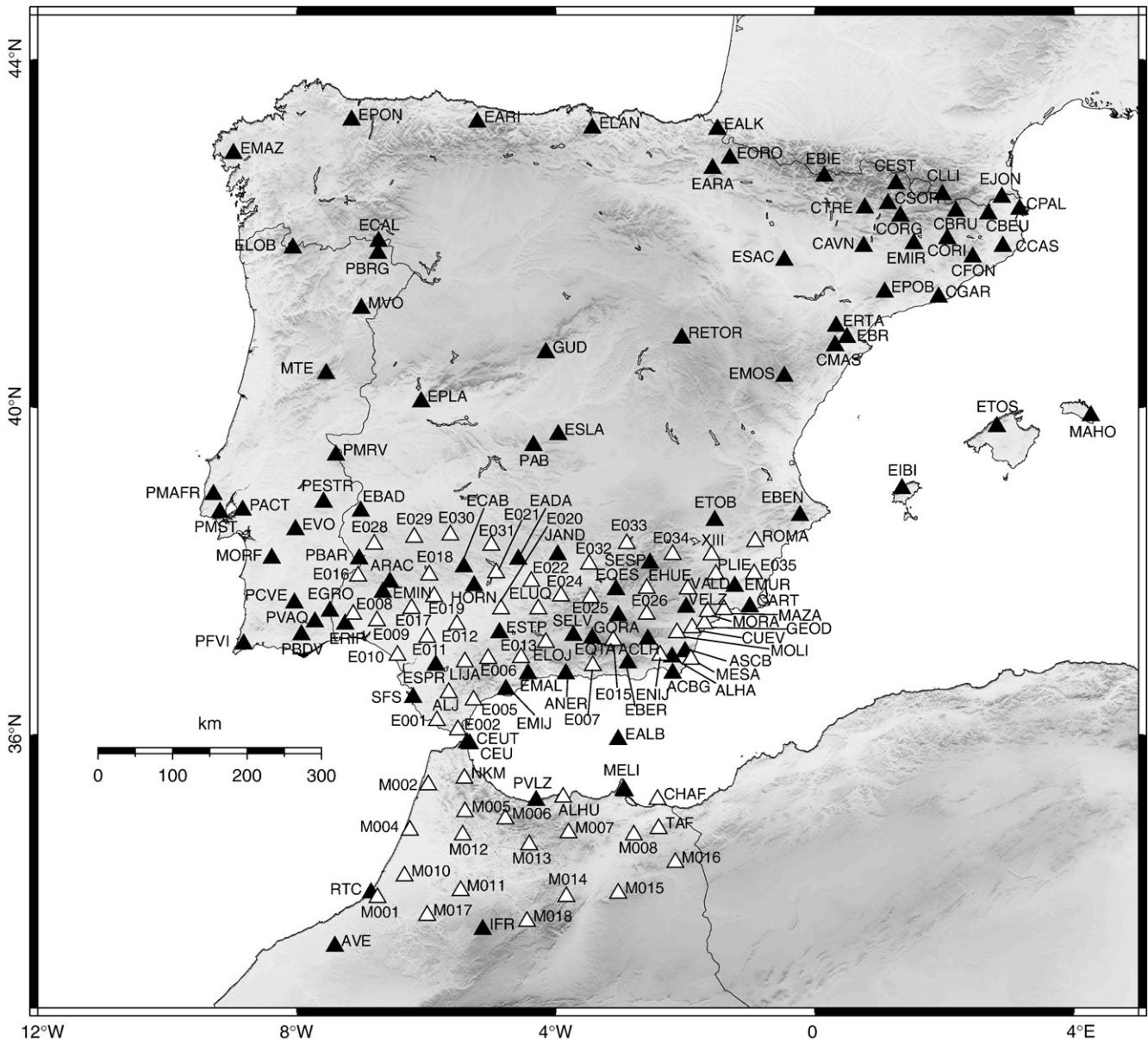

Fig. 1. Distribution of permanent (filled triangles, operated by IGN, IAG, IGC, IM/FCUL, Geofon/ROA/UCM, IST, MedNet, IRIS or Observatori de l'Ebre) and temporary (open triangles, operated by the TopoIberia team or by IAG) seismic broadband stations in the Iberia–Maghreb region in 2008.

Table 1
IAG moment tensor solutions from mid 2005 to end of 2008. Deviatoric moment tensors have been decomposed into a double-couple tensor and residual compensated vector dipole component (CLVD). We give strike, dip and rake of both nodal planes of the double-couple tensor (fault angles in the coordinate system of Aki and Richards, 2002), and the percentage of CLVD remainder.

Date (year/month/day)	Origin time (h:min:s)	Latitude [°N]	Longitude [°E]	Depth [km]	Seismic moment [Nm]	Magnitude Mw	Strike 1 [°]	Dip 1 [°]	Rake 1 [°]	Strike 2 [°]	Dip 2 [°]	Rake 2 [°]	CLVD [%]
2005/06/30	01:19:22	36.65	−1.54	6	$5.90 \cdot 10^{14}$	3.8	63	36	111	218	57	76	5
2005/07/02	12:58:07	35.72	−3.54	6	$2.63 \cdot 10^{15}$	4.2	236	74	60	121	34	150	3
2005/07/06	07:27:05	35.71	−3.53	6	$9.29 \cdot 10^{14}$	3.9	236	77	46	133	45	162	20
2005/07/19	08:04:43	36.26	−11.53	10	$5.58 \cdot 10^{15}$	4.5	204	68	−16	300	74	−157	14
2005/07/20	19:54:07	36.97	0.66	16	$6.24 \cdot 10^{14}$	3.8	191	79	6	100	84	169	11
2005/08/29	09:38:54	36.59	−11.19	40	$9.52 \cdot 10^{15}$	4.6	52	57	99	217	34	77	4
2005/10/24	15:10:57	35.13	−4.02	16	$6.31 \cdot 10^{14}$	3.8	17	82	−14	109	75	−172	13
2005/12/01	20:02:06	40.06	−8.61	12	$2.13 \cdot 10^{14}$	3.5	284	85	−134	189	44	−7	0
2005/12/29	04:25:44	38.88	−8.23	10	$1.98 \cdot 10^{14}$	3.5	104	68	173	196	84	22	12
2005/12/29	05:01:02	38.88	−8.23	8	$3.48 \cdot 10^{14}$	3.7	96	66	167	191	79	24	25
2006/01/10	10:57:40	36.15	−7.71	20	$4.55 \cdot 10^{14}$	3.7	110	78	150	207	61	14	24
2006/01/22	16:27:33	38.51	−6.56	26	$3.68 \cdot 10^{14}$	3.7	76	34	144	198	71	62	9
2006/01/30	07:58:13	35.06	−4.01	14	$2.48 \cdot 10^{15}$	4.2	128	63	−164	31	76	−27	5
2006/03/08	09:04:14	37.71	−1.61	2	$1.74 \cdot 10^{14}$	3.5	242	68	82	83	24	110	6
2006/03/10	19:33:17	40.02	−1.25	6	$3.52 \cdot 10^{15}$	4.3	179	46	−78	343	45	−101	24
2006/03/11	13:43:07	36.87	−4.98	22	$6.92 \cdot 10^{14}$	3.9	243	88	−170	152	80	−2	1
2006/03/26	18:15:40	36.83	−5.04	14	$3.47 \cdot 10^{14}$	3.7	151	70	5	60	85	160	10
2006/04/05	17:22:00	38.17	−1.08	8	$4.16 \cdot 10^{14}$	3.7	253	75	7	162	84	165	6
2006/04/15	19:52:31	39.30	−9.17	26	$2.87 \cdot 10^{14}$	3.6	55	47	85	243	44	96	12
2006/04/23	05:31:36	43.66	−9.03	10	$2.26 \cdot 10^{15}$	4.2	167	85	−35	260	54	−174	8
2006/06/10	06:18:45	42.44	−6.48	20	$1.72 \cdot 10^{15}$	4.1	203	63	6	110	84	153	16
2006/06/21	00:51:16	35.93	−10.47	50	$1.28 \cdot 10^{16}$	4.7	122	57	152	228	67	37	5
2006/07/07	13:13:03	35.40	−9.57	8	$5.35 \cdot 10^{14}$	3.8	279	68	178	9	88	22	36
2006/07/23	20:17:13	35.69	0.74	6	$5.56 \cdot 10^{15}$	4.5	61	39	113	213	55	73	13
2006/07/23	23:07:00	35.81	0.68	8	$7.50 \cdot 10^{14}$	3.9	76	29	95	250	61	87	16
2006/08/10	09:16:07	35.50	−9.91	50	$4.30 \cdot 10^{15}$	4.4	21	83	8	290	82	173	25
2006/11/17	18:19:51	42.96	−0.15	6	$7.97 \cdot 10^{15}$	4.6	105	35	−84	279	55	−94	11
2006/12/16	19:34:34	36.45	0.91	8	$6.08 \cdot 10^{15}$	4.5	62	17	114	217	74	83	9
2007/01/02	12:19:26	37.11	−5.39	10	$2.98 \cdot 10^{14}$	3.6	135	79	−174	44	84	−10	19
2007/01/02	15:00:47	37.16	−5.33	14	$3.24 \cdot 10^{14}$	3.6	136	71	−152	37	64	−21	22
2007/01/04	23:32:32	37.19	−3.77	6	$3.57 \cdot 10^{14}$	3.7	303	53	−62	83	44	−121	1
2007/02/12	10:35:22	35.90	−10.31	50	$9.86 \cdot 10^{17}$	6.0	122	55	147	232	63	40	1
2007/05/08	06:56:34	36.16	2.54	16	$4.83 \cdot 10^{15}$	4.4	137	84	−133	41	43	−7	11
2007/06/09	07:15:16	37.06	−3.63	12	$1.34 \cdot 10^{14}$	3.4	188	38	−55	327	59	−114	8
2007/06/27	01:22:10	36.56	5.39	2	$8.95 \cdot 10^{15}$	4.6	148	2	160	258	89	88	23
2007/06/30	03:53:45	37.07	−5.44	8	$3.88 \cdot 10^{14}$	4.4	81	45	123	218	53	61	6
2007/06/30	11:29:35	37.08	−5.42	8	$3.06 \cdot 10^{14}$	3.6	103	58	158	205	71	34	13
2007/08/11	20:45:58	33.19	−5.31	20	$1.23 \cdot 10^{16}$	4.7	106	87	171	197	81	3	16
2007/08/12	07:47:05	39.35	−2.99	12	$1.33 \cdot 10^{16}$	4.7	335	85	6	244	84	175	1
2007/08/22	18:08:33	36.03	2.77	4	$5.15 \cdot 10^{15}$	4.4	23	57	−1	114	88	−147	3
2007/09/03	13:21:16	37.32	−1.88	8	$1.44 \cdot 10^{14}$	3.4	26	73	18	290	72	162	13
2007/09/08	16:41:30	35.68	−3.49	4	$4.63 \cdot 10^{15}$	4.4	259	64	78	104	28	113	10
2007/09/14	03:45:06	37.08	−5.47	12	$2.39 \cdot 10^{14}$	3.6	65	35	107	224	56	78	15
2007/09/14	03:46:49	37.08	−5.47	8	$2.67 \cdot 10^{14}$	3.6	51	54	97	220	36	81	3
2007/09/18	23:20:42	37.01	−5.43	8	$8.57 \cdot 10^{14}$	3.9	52	34	103	217	57	82	3
2007/10/01	00:39:56	37.05	−3.93	6	$2.22 \cdot 10^{14}$	3.5	107	62	−120	338	40	−46	7
2008/01/09	22:24:02	35.64	−0.64	6	$1.17 \cdot 10^{16}$	4.7	61	18	108	223	73	84	18
2008/01/11	00:21:46	36.49	−9.99	50	$5.88 \cdot 10^{15}$	4.5	33	73	42	289	50	158	17
2008/02/06	17:53:01	36.99	−2.20	12	$2.27 \cdot 10^{15}$	4.2	12	84	5	281	85	174	8
2008/02/25	15:29:53	42.62	−9.22	10	$2.33 \cdot 10^{14}$	3.5	76	69	146	180	59	25	9
2008/03/02	04:03:52	37.95	−0.90	4	$1.93 \cdot 10^{14}$	3.5	298	73	113	63	28	38	12
2008/04/28	05:25:05	39.71	−3.46	6	$3.09 \cdot 10^{14}$	3.6	42	89	−140	311	50	0	11
2008/04/30	22:30:40	38.15	−1.70	8	$1.25 \cdot 10^{14}$	3.4	324	73	165	59	76	18	4
2008/05/10	16:33:09	35.97	−10.77	50	$6.92 \cdot 10^{14}$	3.9	360	77	−88	174	13	−95	11
2008/05/18	01:57:21	43.10	−0.12	8	$5.03 \cdot 10^{14}$	3.8	256	61	−102	100	31	−68	8
2008/06/06	20:02:57	35.88	−0.69	10	$2.22 \cdot 10^{17}$	5.5	51	19	98	222	71	87	2
2008/06/06	22:48:23	35.83	−0.63	6	$1.92 \cdot 10^{15}$	4.2	62	17	117	215	75	82	20
2008/06/15	20:55:24	39.02	−0.42	6	$8.96 \cdot 10^{13}$	3.3	164	45	−101	358	46	−79	27
2008/06/18	13:23:58	36.19	1.15	8	$7.33 \cdot 10^{15}$	4.5	38	32	77	233	59	98	1
2008/07/17	19:22:07	36.24	−9.89	60	$8.24 \cdot 10^{14}$	3.9	20	51	62	240	47	120	16
2008/07/21	02:30:03	39.01	−0.42	6	$3.46 \cdot 10^{14}$	3.7	155	41	−120	13	55	−65	1
2008/07/22	22:36:32	41.85	2.61	6	$3.26 \cdot 10^{14}$	3.6	169	63	−97	5	28	−75	6
2008/07/24	17:19:52	35.64	−0.98	10	$4.47 \cdot 10^{15}$	4.4	60	18	85	245	72	92	2
2008/08/16	10:21:20	41.37	3.06	14	$1.55 \cdot 10^{14}$	3.4	50	66	37	303	57	150	0
2008/08/24	20:52:44	36.45	1.05	4	$5.71 \cdot 10^{14}$	3.8	56	14	103	222	76	87	17
2008/09/14	14:03:39	38.27	−0.90	4	$4.45 \cdot 10^{14}$	3.7	148	51	160	251	74	41	2
2008/10/02	04:02:53	37.04	−5.42	4	$6.89 \cdot 10^{15}$	4.5	54	44	103	216	47	78	1
2008/10/02	04:05:06	37.02	−5.43	12	$9.17 \cdot 10^{14}$	3.9	54	39	92	232	51	88	13
2008/10/02	05:14:19	37.06	−5.43	6	$1.19 \cdot 10^{14}$	3.4	44	45	109	198	48	72	4
2008/10/02	09:22:14	37.06	−5.40	16	$7.66 \cdot 10^{13}$	3.2	87	66	166	183	77	25	7
2008/10/08	16:04:47	37.06	−5.41	12	$2.11 \cdot 10^{14}$	3.5	211	69	24	111	68	157	5
2008/10/20	09:46:11	36.49	−2.57	6	$4.50 \cdot 10^{14}$	3.7	16	73	−42	120	49	−158	29

Table 1 (*continued*)

Date (year/month/day)	Origin time (h:min:s)	Latitude [°N]	Longitude [°E]	Depth [km]	Seismic moment [Nm]	Magnitude Mw	Strike 1 [°]	Dip 1 [°]	Rake 1 [°]	Strike 2 [°]	Dip 2 [°]	Rake 2 [°]	CLVD [%]
2008/10/21	03:28:53	36.47	−2.56	14	$3.05 \cdot 10^{15}$	4.3	112	62	−174	19	85	−27	11
2008/10/21	05:55:46	36.47	−2.59	14	$3.29 \cdot 10^{15}$	4.3	114	72	−168	20	78	−18	7
2008/10/21	12:50:56	36.47	−2.52	14	$6.29 \cdot 10^{14}$	3.8	21	75	−11	114	79	−165	0
2008/10/26	00:51:22	36.47	−2.57	14	$1.30 \cdot 10^{15}$	4.0	22	79	−12	115	78	−169	7
2008/11/07	11:02:51	36.47	−2.57	6	$3.92 \cdot 10^{15}$	4.4	128	57	−148	19	64	−36	3

1982; Herrmann and Wang, 1985). For moment tensor inversion, we compute reflectivity Greens functions (Randall et al., 1995) for several plane layered earth structures representative of the Iberia–Maghreb lithosphere (Stich et al., 2003) and invert observed displacement seismograms with a least squares technique to obtain the five independent components of the deviatoric moment tensor. Moment tensor inversion is combined with a grid search over focal depths (with increments of 2 km in the crust and 10 km in the upper mantle) to retrieve the formally best combination of centroid depth and moment tensor. This procedure allows for obtaining an independent estimate of focal depth, assessing the stability of the solution, and reducing the impact of errors in routine hypocenter locations on the moment tensor estimates.

We use complete three-component seismograms for moment tensor analysis in order to include all available polarity and amplitude information from regional body and surface waves. Waveforms are filtered in an intermediate period band, restricting the inversion to wavelengths that are less prone to complicate propagation effects introduced by lithospheric heterogeneity. We use filter bands of usually 20 s to 50 s for magnitude 4+ events, and 15 s to 35 s for smaller events that have too low signal-to-noise ratio at longer periods. For the shorter band, the most useful waveforms correspond to near-regional distance stations out to ~300 km, while at longer distances crustal heterogeneity may complicate an accurate wave-form matching for surface waves. A careful manual processing is applied to control the inversion result. This involves an interactive tuning of weighting factors for individual traces and the visual inspection of waveform matches, to ensure that the moment tensor estimate reproduces the key features in recorded waveforms, or to reject unsatisfactory and unstable solutions otherwise. Finally, the deviatoric moment tensor is decomposed into a double-couple tensor and a residual compensated linear vector dipole (CLVD, Jost and Herrmann, 1989), and the double-couple part is used to infer the orientation of nodal planes and principal strain axes.

We consider for this study earthquakes from May 2005 to December 2008 with reported magnitudes ≥4 for remote regions like Algeria or the Atlantic Ocean, ≥3.5 for the Iberian Peninsula, northern Morocco and adjacent offshore areas, and ≥3.2 for areas of particularly dense instrumentation like southern Spain. We were able to obtain stable moment tensor solutions for 77 events (Table 1). Moment magnitudes range from 3.2 to 6.0, and centroid depths from 2 km to 60 km. All earthquakes below Moho depth are located west of 9.5°W within oceanic lithosphere in the Atlantic. The average CLVD remainder is 10%, and we interpret moment tensors in terms of simple shear faulting throughout. The largest event of this catalogue update is the Mw 6.0, 12 February 2007 earthquake offshore Cape St. Vincent, that provides information on the characteristics of faulting in the oceanic upper mantle offshore Portugal, and has been discussed pre-viously in the context of the great 1755 Lisbon earthquake (Stich et al., 2007). We present here the inversion result for the second largest earthquake (Mw = 5.5, 6 June 2008, near Oran in northwestern Algeria, Fig. 2). This event was recorded with good signal quality at stations over the entire Iberia–Maghreb region, and we used 80 three-component waveforms for moment tensor inversion. We obtain a minimum fractional misfit and a minimum CLVD component for a centroid depth of 10 km, and a near double-couple reverse faulting

solution with strike of the preferred nodal plane of N51°E, dip 19° and rake 98°. A good correspondence between observed and predicted waveforms (Fig. 2) confirms a good performance of our average earth models for 20–50 s waveforms and many regional paths, and supports credibility of the moment tensor estimate.

At the other end of the magnitude range, 45 events (58%) of this catalogue update correspond to earthquakes with moment magnitude less than 4 (Mw 3.2 to 3.9). This is a significantly larger percentage compared to the previous IAG solutions for 1984–2005 (31% of Mw<4 earthquakes), confirming the power of the dense station network to resolve source radiation from small earthquakes. Yet, the level of completeness in this period range is clearly lower than for magnitude 4+ events, and the success of moment tensor inversion for events around Mw 3.5 depends critically on the source location (through the varying local station density and complexity of the near-source Earth structure) and instantaneous atmospheric conditions (through noise introduced by pressure fluctuation, that can frequently exceed the intermediate period signal generated by small earthquakes). We show as a successful example the inversion of the Mw 3.4, 30 April 2008 Calasparra, Murcia earthquake, based on 12 selected near-regional recordings from IAG, IGN and Geofon stations between 55 km and 185 km epicentral distance (Fig. 3). We obtained centroid depth of 6 km, a CLVD component of 1%, and a strike-slip faulting mechanism with a minor reverse slip component and a sub-horizontal, N11°E orientation of the moment tensor P-axis. Fractional least squares misfit is clearly larger than in the previous example due to the relevant noise content in the traces, but a visual inspection of waveform matches shows that practically all features that emerge from the background noise are fitted appropriately, suggesting suitability of this solution for the moment tensor catalogue.

3. Discussion of new moment tensor solutions

The general seismotectonic framework of the Iberia–Maghreb region is conditioned by the oblique NW–SE to WNW–ESE conver-gence between the African (Nubian) and Eurasian plates at a rate of ~5 mm/year (DeMets et al., 1994; Calais et al., 2003; McClusky et al., 2003, Serpelloni et al., 2007; Fernandes et al., 2007). A consistent, simple pattern of ~NW–SE directed thrust earthquakes can be found at the Mediterranean margin of Algeria (Bezzeghoud and Buforn, 1999; Pondrelli et al., 2002; Braunmiller and Bernardi, 2005; Stich et al., 2006). Similar NW–SE reverse faulting mechanisms were also reported for several moderate to large earthquakes in and around Portugal, like the 1909 Mw 6.0 Benavente earthquake (Stich et al., 2005c) and the 1969 Mw 7.8 Horseshoe earthquake (Fukao, 1973), and generally seismotectonic deformation west of the Strait of Gibraltar is characterised by a transpressional regime (e.g. Grimison and Chen, 1986; Buforn et al., 1988, Sartori et al., 1994; Stich et al., 2005a). Between the Algerian and Portuguese margins, in the area comprising northern Morocco, the Alboran Sea and Southern Spain, the complexity of plate boundary deformation increases significantly, with most available stress indicators (Fernández-Ibáñez et al., 2007) showing no obvious relationship to the ongoing plate convergence, but rather responding to the superposition of extensional tectonics in the Alboran Basin (e.g. Mezcua and Rueda, 1997; Stich et al., 2006). Also in part of eastern Spain, normal faulting is the dominant
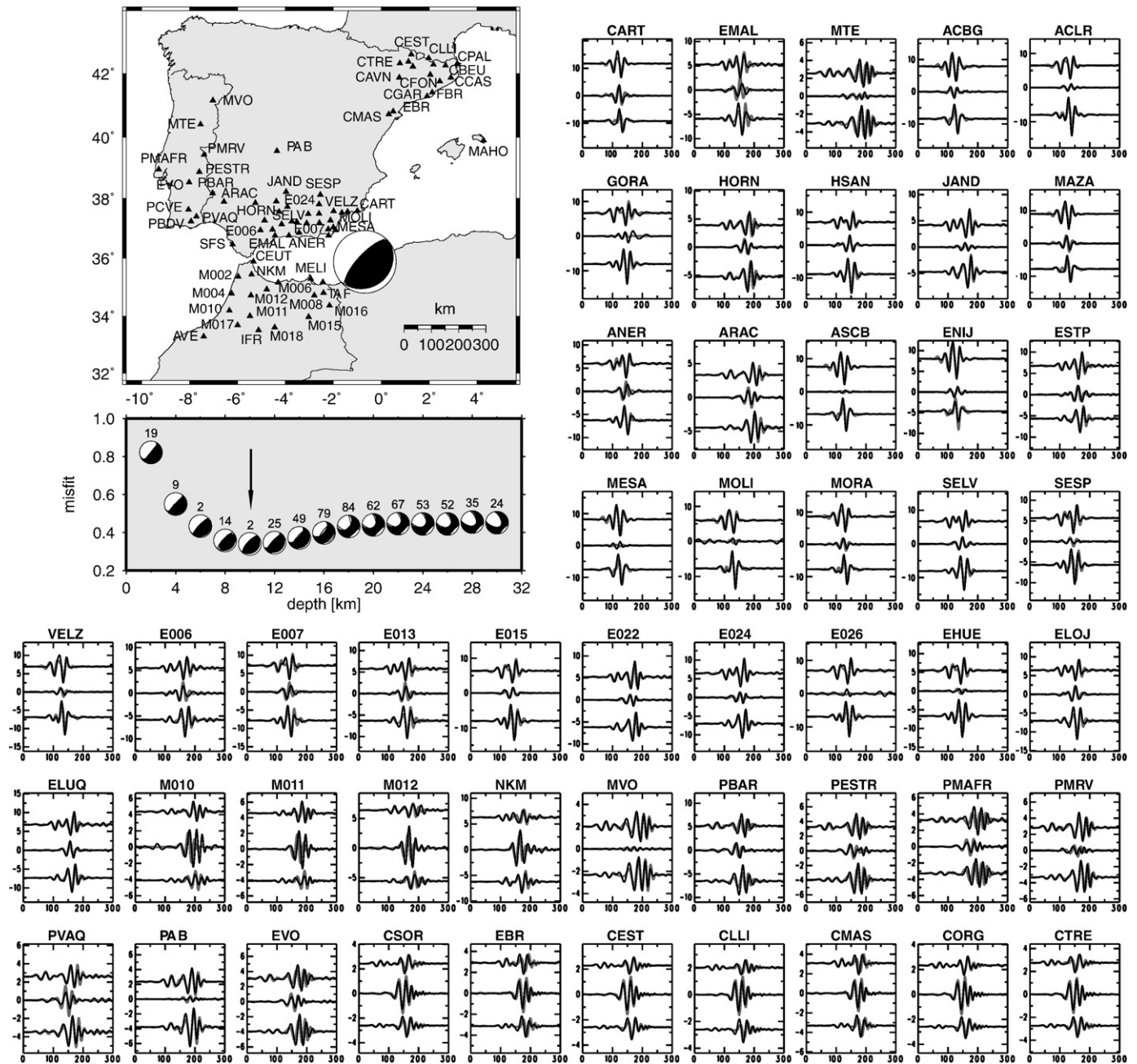
Fig. 2. Moment tensor inversion result for the Mw 5.5, 6 June 2008, Oran, Algeria earthquake. The map shows the location of 79 stations analyzed and the best solution in equal-area, lower hemisphere projection. Not all station codes could be labeled due to the size of the map. Waveform matches are shown for 50 stations, with observed seismograms in black and moment tensor predictions in grey. In each station panel, the radial, transverse and vertical components of displacement are plotted from top to bottom. Displacement is given in 10^{-5} m and time in seconds. We further show the inversion result for different trial depths, indicating minimum misfit and minimum CLVD component (small numbers above mechanisms) at 10 km depth.

earthquake mechanism, and tectonics appears to be controlled by the opening of the western Mediterranean Basin rather than by plate convergence.

Coeval extension within the convergent Iberia–Maghreb plate boundary zone is generally attributed to dynamic upper mantle processes, representing the late state of the evolution of the western Mediterranean subduction system (Faccenna et al., 2004). In the Alboran domain, upper mantle dynamics are manifested in the occurrence of intermediate and deep earthquakes and velocity anomalies in tomographic images (e.g. Calvert et al., 2000), but the underlying mechanism is still discussed controversially. Geodynamic models range from convective removal and delamination to active oceanic or continental subduction (e.g. Platt and Vissers, 1989;

Docherty and Banda, 1995; Seber et al., 1996, Lonergan and White, 1997; Morales et al., 1999; Gutscher et al., 2002). Westward oceanic subduction beneath the arc of Gibraltar (Gutscher et al., 2002; Gutscher, 2004) could not be supported by GPS measurements yet (Stich et al., 2006), while recent GPS data from northern Morocco (Fadil et al., 2006; Tahayt et al., 2008) resolve relative motion of tectonic blocks in the Rif mountain belt, insinuating that upper mantle dynamics may involve continental type lithosphere. Similarly, in the western Betic mountain range (southern Spain) a continental slab has been proposed based on tomographic and gravimetric evidence (Morales et al., 1999), but this apparent symmetry would not necessarily imply identical driving mechanisms (subduction vs. delamination) on either side of the Alboran Basin. The eastern
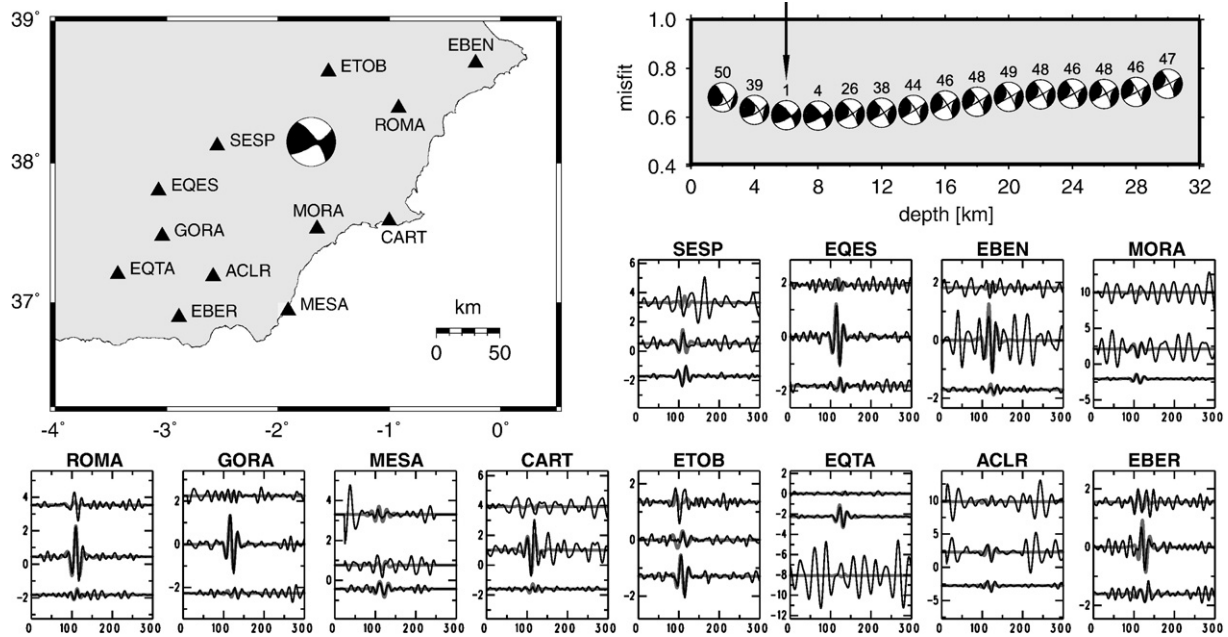
Fig. 3. Moment tensor inversion result for a small earthquake (Mw 3.4), on 30 April 2008 near Calasparra, Murcia. 12 near-regional recordings are used. The signal to noise level is low and not all components can be used in inversion, but all main features in the waveforms are predicted adequately by the moment tensor solution. Representation of map, misfit-depth curve and waveform matches as in Fig. 2, except for displacement being given in 10^{-7} m for this smaller earthquake.

boundary of the Alboran domain is marked by the left-lateral Betic–Alboran shear zone (Bousquet, 1979; Gutscher 2004; Stich et al., 2006), expressed as a belt of intense earthquake activity following the SE-Spanish coast and crossing over the Alboran Sea to the Moroccan margin, with an overall NE–SW trend.

Published seismic source estimates for the Iberia–Maghreb plate boundary region (e.g. Buforn et al., 2004, Stich et al., 2006) are generally consistent with information derived from geological and geodetic studies; however they still lack coverage along several sections of the plate boundary zone as well as in foreland areas. A relevant characteristic of this catalogue update, owing to a fortunate geographical distribution of recent seismic activity and our capability to include small earthquakes into moment tensor analysis, is the fact that new solutions fill several of the gaps in the previous focal mechanism inventory (Fig. 4). For example, 17 mechanisms were obtained north of 38.5°N, shedding more light on intraplate deformation in the Iberian Peninsula. Below, we discuss situations where the new mechanisms significantly complement or extend our image of regional seismotectonics. The new mechanisms are referenced in the text and in Fig. 4 using a 6-digit code composed of the year, month and day of occurrence, and a capital letter A–D where necessary to distinguish several catalogue solutions for the same day according to the temporal order of the events.

3.1. NW-Algeria

Along the NW-Algerian Mediterranean margin (west of 2°E) nine new mechanisms (Mw 3.8–5.5) were obtained, significantly extending the previous dataset of four mechanisms in the IAG catalogue. Earthquake sources along the NW-Algerian margin are associated primarily with shallow, landward-dipping thrust faults, as is also the case for the central Algerian margin (2°E–6°E) with the well studied Mw 6.9, 2003 Bourmedes earthquake sequence (Braunmiller and Bernardi, 2005). The difference between both regions consists in the orientation of P-axes, which show a NNW azimuth at the central Algerian Margin, and a noticeably different, NW-azimuth at the western margin (with the exceptions of events 060723B and 080724, that show shortening directions similar to the central Algerian margin). The rotation corresponds to a similar rotation in the strike

of the coastline. The SE–NW compression at the western part of the margin is closer to the geodetically derived NW–WNW motion of the Nubian plate with respect to stable Europe (DeMets et al., 1994; Serpelloni et al., 2007), compared to the central part of the margin. This situation represents regional-scale slip partitioning, with thrusting at the western Algerian margin being perpendicular to the strike of the left-lateral Betic–Alboran shear zone, as discussed in the following section. Note that the left-lateral sense of shear is opposite to the motion expected for slip partitioning under plate convergence, providing evidence for a secondary stress source in the Alboran domain (Stich et al., 2006, Fernández-Ibáñez et al., 2007).

3.2. Betic–Alboran shear zone

Moment tensor estimates for the Betic–Alboran shear zone show the expected dominance of strike-slip faulting, and occasional normal and reverse faulting earthquakes with orientations consistent with the average stress field (Stich et al., 2006). In this update we were able to include new earthquakes from the vicinity of the Carboneras and Palomares fault zones (36.5°N to 37.5°N), although none of the events can be associated to the main fault traces. Those mechanisms (070903, 080206, 081020, 081021A-C, 081026, 081107) are remarkably similar, showing nearly strike-slip faulting style with NNE–SSW oriented left-lateral and WNW-ESE oriented right-lateral nodal planes. Depth estimates range from 6 to 14 km. The left-lateral planes show a ~N20°E trend, which is similar to the Palomares fault and ~30° rotated with respect to the Carboneras fault zone, but we have no complementary information yet to distinguish between the primary fault and auxiliary nodal planes. In Morocco, we obtained three strike-slip earthquakes (051024, 060130, 070811), similar to the solutions near the Carboneras fault as well as of most of the aftershocks of the 2004 Al Hoceima earthquake (Stich et al., 2005b). Three offshore earthquakes with predominately reverse slip (050702, 050706, 070908) occurred at the Alboran ridge (Comas et al., 1999), where occasional reverse slip components in strike-slip mechanisms have been observed previously (Stich et al., 2006).

Within our moment tensor inventory for the Betic–Alboran shear zone, there was a sort of gap between 38°N and 39°N, in the Alicante region. This gap separated two well-sampled areas with a dominance
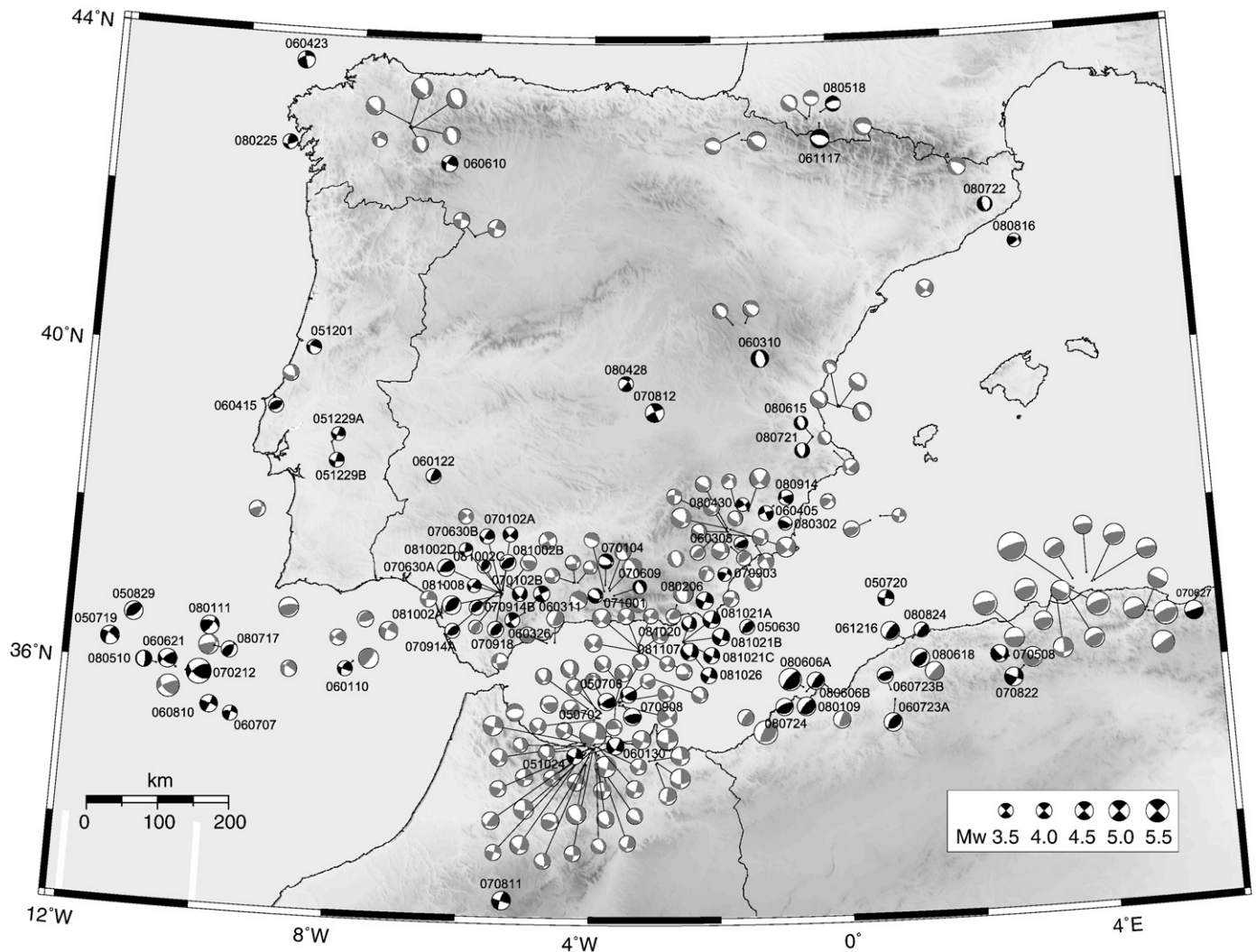
Fig. 4. New moment tensor solutions (with compressional quadrants in black) and previous solutions in the IAG catalogue (grey). The double couple tensor is plotted in lower hemisphere projection. The new mechanisms are referenced using the year, month and day of occurrence, and, where necessary, a capital letter A–D to distinguish several catalogue solutions for the same day according to the temporal order of the events (compare to Table 1).

of strike-slip faulting to the south and west, and a dominance of normal faulting to the north, while offshore mechanisms along this sector pointed to a more compressive local deformation style. The Alicante region is the northern termination of the east Betic shear zone, with the ~N70–80°E striking Crevillente and Bajo Segura faults as the dominant structures (e.g. Alfaro et al., 2002). Although in this update only three solutions for this area could be provided (060405, 080302, 080914), now a consistent pattern starts to emerge. Moment tensors show strike-slip to reverse faulting style, similar to the older offshore solutions, but contrasting with both the strike-slip and normal faulting style observed to the south and north respectively. This indicates that the Alicante area acts as a backstop for shear deformation along the SE-Spanish margin, accommodating residual compression on the eastern side of the shear zone, and separating shear deformation from the ~ENE–WSW extensional deformation style further north. One oblique mechanism (080914) is located on the Crevillente fault, at 4 km depth, and has a nodal plane coincident with the strike of the fault (strike N251°E, dip 74°, rake 41°). While the small magnitude (Mw 3.7) does not allow us to assign this event unambiguously to the main fault, it may well be a hint on the current kinematics of the fault zone. Another reverse faulting mechanism (060308) occurred close to the Alhama de Murcia fault, consistent with geological observations of a compressional component of deformation along this structure (Martínez-Díaz, 2002, Masana et al., 2004).

3.3. Betic Cordillera

Within the Betic Cordillera faulting style changes from predominately strike-slip in the east Betic shear zone towards predominately normal faulting in the central Betics. Normal faulting mechanisms are generally in geographical proximity to Neogene intramountain basins and indicate ENE–WSW extension (Galindo-Zaldívar et al., 1999; Stich et al., 2006). Three more normal faulting mechanisms were obtained beneath and around the Granada basin (070104, 070609, 071001), confirming this pattern. In the Western Betics, only two moment tensor mechanisms have been available previously, not being sufficient for establishing the characteristics of seismotectonic deformation. Since 2006, however, several seismic sequences have affected this area, allowing for the computation of 14 new moment tensor solutions (060311, 060326, 070102A-B, 070630A-B, 070914A-B, 070918, 081002A-D, 081008, Mw 3.2–4.5). Faulting style in the Western Betics is clearly different from the central Betics, showing reverse to strike-slip solutions. In the context of the Betics, these mechanisms are located close to the external mountain front, while seismicity further east is located in the interior of the Betic chain. This can be interpreted as activity of the NW-Betic mountain front, oriented favorably to regional plate convergence, as opposed to inactivity of the N-Betic mountain front, where normal faulting affects the internal zones of the chain (Ruiz-Constán et al., 2009). In a

regional context, we observe similarity of these mechanisms to solutions from the foreland and the Atlantic (discussed next), which suggests an overall change of faulting style at ~5°W. A remarkable degree of heterogeneity is apparent in our solutions for the western Betics, including strike-slip faulting mechanisms with opposite kinematics.

3.4. Western and central Iberia

This area, comprising the Iberian Massif and the central Portuguese-Galician Atlantic margin, provides the most remarkable example of how the catalogue update affects our view of regional seismotectonics. While first regional moment tensor solutions still pointed to a complete dominance of normal faulting over the entire central and northern part of the Iberian Peninsula, indicating a NE–SW extensional stress regime (Stich et al., 2003), the recent solutions increase our coverage significantly and provide a more differentiated picture. In fact, along the Pyrenees, the Iberian Chain and the Valencia coast, normal faulting remains the only mechanism, accounting for all 18 solutions in the catalogue. In contrast, in the central and western part of the Iberian Peninsula the current moment tensor inventory evolves towards a dominance of strike-slip faulting, often with a minor reverse slip component. Two new reverse faulting solutions (060122, 060415) show a ~N320°E orientation of P-axes, similar to the reverse faulting solution for the Mw 6.0, 1909, Benavente, Portugal earthquake (Stich et al., 2005c). The new solutions bring the seismological evidence in better agreement to recent stress field estimates in western Iberia, indicating predominantly strike-slip faulting conditions (De Vicente et al., 2008). Further, a clear similarity between onshore SW-Iberia and offshore faulting in the Atlantic (next section) becomes apparent, suggesting similar style and orientation of tectonic deformation in both domains.

3.5. SW-Portuguese margin

The recent densification of the seismic broad band network in Portugal proved very useful to address offshore earthquakes at the SW-Portuguese Atlantic margin. Nine more solutions could be provided for the area west of 9.5°W, significantly increasing the previous inventory of two solutions in the IAG catalogue for this sector. One new solution (060110) was obtained for the Gulf of Cadiz. Faulting characteristics are similar in the Gulf of Cadiz and Cape St. Vincent area, and resemble the situation in SW-Iberia including the western Betics. Earthquakes occur predominately as reverse and strike-slip faulting events. A relevant property of faulting at the SW-Iberian margin is the depth distribution of earthquakes, with 7 of the new solutions located at sub-Moho depths between 40 and 60 km, among them the largest event of this catalogue update, the Mw 6.0, 12 February 2007 earthquake. This indicates coupling between the crustal and upper mantle strain fields in the oceanic lithosphere (Stich et al., 2005a). This also has important implications for seismic and tsunami hazard, since earthquake rupture can propagate in the brittle uppermost mantle, where high rigidity may contribute to larger than average stress drops, and the large downdip extend of mature faults may be responsible for large earthquakes like the 1755, Mw 8.5–8.7, Lisbon earthquake (Stich et al., 2007). Also here we observe heterogeneity of faulting, with the most remarkable example being a pure normal faulting, Mw 3.9 earthquake (080510). This event occurred at 50 km depth and is not straightforward to interpret in the regional seismotectonic context. However, faulting depth and mechanism for this event is in good agreement with results from local data analysis using OBS array observations (Geissler et al., 2009), and two more upper mantle normal faulting earthquakes have been reported previously (Stich et al., 2005a).

4. Conclusion

Two of the most promising approaches to increase the amount and reliability of moment tensor estimates for small earthquakes are apparently the use of a dense regional recording network (e.g. Braunmiller et al, 2002; Clinton et al., 2006), and the use of more realistic three-dimensional earth models to calculate moment tensor Greens functions numerically (e.g. Liu et al., 2004). While an appropriate 3D reference model is not yet available for the Iberia–Maghreb region, the densified network of permanent stations and present portable deployments produce a large amount of high quality recordings at short epicentral distance and allow for inverting small events based on near-regional recordings and 1D Greens functions. The dense coverage allows for sorting out traces affected by noise, or stations where average 1D models may be not appropriate to predict real propagation effects. Also, the large amount of waveforms available for individual inversions in general increases our confidence in the moment tensor estimates, assuming that an appropriate fit to waveforms at many different azimuths and distances should not be a coincidence. We could obtain a substantial update of the Iberia–Maghreb moment tensor inventory of 77 solutions from mid 2005 to the end of 2008. The percentage of Mw <4 solutions in this update (58%) nearly doubled with respect to the previous IAG moment tensor solutions (31%), or the current IGN near real-time catalogue (30%). Due to the possibility of including small events, and the geographical distribution of recent seismicity, this update achieves a significant improvement of our image of regional faulting patterns.

Among the areas where the new moment tensors contribute to a better understanding of regional seismotectonics, we discussed the NW-Algerian margin, the Betic–Alboran shear zone, the western Betics, the Atlantic, and the Iberian massif. Along the Algerian Mediterranean margin, new moment tensors reveal a rotation of the shortening direction from ~NNW–SSE in the eastern part to ~NW–SE in the western part. In the Betic–Alboran shear zone, new moment tensors reproduce the compressive strains at the northern termination of the shear zone, coincident with information from geologic studies. In the western Betics, new mechanisms show strike-slip and reverse faulting, in significant contrast to the hegemony of normal faulting in the central Betics. Faulting style and orientation in the foreland (Iberian massif) and in the Atlantic offshore from the SW-Portuguese margin are very similar to the western Betics. In the latter area however, earthquakes show a different depth distribution, extending into the brittle uppermost oceanic mantle down to ~50 km.

On the other hand, the updated moment tensor catalogue is still insufficient for example to establish the characteristics of faulting in NE-Spain, where only few and heterogeneous mechanisms are available, as well as in the vicinity of the Strait of Gibraltar, probably in a key position for our understanding of regional geodynamics. Another conspicuous feature of the catalogue is the heterogeneity of solutions for the western Betics, Iberian massif and the SW-Portuguese margin. This heterogeneity includes for example strike-slip mechanisms with opposite kinematics, or upper mantle normal faulting within a transpressional environment, with both examples being well supported by the data. Heterogeneity indicates varying local stress conditions, and points to fault interaction, meaning that local tectonics play an important role in understanding regional deformation. Especially low magnitude earthquakes may be prone to activation under local stress conditions. Nevertheless, further east we observe that mechanisms are more homogeneous locally, and slip partitioning appears to happen at regional scale, for example through thrusting in northern Algeria perpendicular to the Betic–Alboran shear zone. A better understanding of heterogeneous and homogeneous faulting patterns, as well as the continued lack of solutions in several areas, is motivation for further efforts to augment the regional moment tensor inventory.

Acknowledgements

References

Aki, K., Richards, P.G., 2002. Quantitative Seismology, 2nd edition. University Science Books, New York.

Alfaro, P., Andreu, J.M., Delgado, J., Estevez, A., Soria, J.M., Teixido, T., 2002. Quaternary deformation of the Bajo Segura blind fault (eastern Betic Cordillera, Spain) revealed by high-resolution reflection profiling. Geol. Mag. 139, 331–341.

Bezzeghoud, M., Buforn, E., 1999. Source parameters of the 1992 Melilla (Spain, Mw = 4.8), 1994 Alhoceima (Morocco, Mw = 5.8), and 1994 Mascara (Algeria, Mw = 5.7) earthquakes and seismotectonic implications. Bull. Seismol. Soc. Am. 89, 359–372.

Bousquet, J.C., 1979. Quaternary strike-slip faults in southeastern Spain. Tectonophysics 52, 277–286.

Braunmiller, J., Bernardi, F., 2005. The 2003 Boumerdes, Algeria earthquake: regional moment tensor analysis. Geophys. Res. Lett. 32, L06305. doi:10.1029/2004GL022038.

Braunmiller, J., Kradolfer, U., Baer, M., Giardini, D., 2002. Regional moment tensor determination in the European–Mediterranean area — initial results. Tectonophysics 356, 5–22.

Buforn, E., Udías, A., Colombas, M., 1988. Seismicity, source mechanisms and tectonics of the Azores–Gibraltar plate boundary. Tectonophysics 152, 89–118.

Buforn, E., Sanz de Galdenao, C., Udías, A., 1995. Seismotectonics of the Ibero-Maghrebian region. Tectonophysics 248, 247–261.

Buforn, E., Bezzeghoud, M., Udías, A., Pro, C., 2004. Seismic sources on the Iberia–African plate boundary and their tectonic implications. Pure Appl. Geophys. 161, 623–646.

Calais, E., DeMets, C., Nocquet, J.M., 2003. Evidence for a post-3.16-Ma change in Nubia-Eurasia-North America plate motions. Earth Planet. Sci. Lett. 216, 8–92.

Calvert, A., Sandvol, E., Seber, D., Barazangi, M., Roecker, S., Mourabit, T., Vidal, F., Alguacil, G., Jabour, N., 2000. Geodynamic evolution of the lithosphere and upper mantle beneath the Alboran region of the western Mediterranean: constraints from travel time tomography. J. Geophys. Res. 105, 10871–10898.

Cesca, S., Buforn, E., Dahm, T., 2006. Amplitude spectra moment tensor inversion of shallow earthquakes in Spain. Geophys. J. Int. 166, 839–854.

Clinton, J.F., Hauksson, E., Solanki, K., 2006. An evaluation of the SCSN moment tensor solutions: robustness of the Mw magnitude scale, style of faulting, and automation of the method. Bull. Seismol. Soc. Am. 96, 1689–1705.

Comas, M.C., Platt, J.P., Soto, J.I., Watts, A.B., 1999. The origin and tectonic history of the Alboran Basin: insights from Leg 161 results. In: Zahn, R., Comas, M.C., Klaus, A. (Eds.), Proc. ODP, Sci. Res., vol. 161. Ocean Drilling Program, College Station, TX, pp. 555–580.

DeMets, C., Gordon, R.G., Argus, D.F., Stein, S., 1994. Effect of recent revisions to the geomagnetic reversal time scale on estimates of current plate motions. Geophys. Res. Lett. 21, 2191–2194.

De Vicente, G., Cloetingh, S., Muñoz-Martín, A., Olaiz, A., Stich, D., Vegas, R., Galindo-Zaldívar, J., Fernández-Lozano, J., 2008. Inversion of moment tensor focal mechanisms for active stresses around the Microcontinent Iberia: tectonic implications. Tectonics 27. doi:10.1029/2006TC002093.

Díaz, J., Villaseñor, A., Gallart, J., Morales, J., Pazos, A., Córdoba, D., Pulgar, J., García-Lobón, J.L., Harnafi, M., Group, TopoIberia Seismic Working, 2009. The IBERARRAY broadband seismic network: a new tool to investigate the deep structure beneath Iberia. Orfeus Newsl. 8, 2.

Docherty, C., Banda, E., 1995. Evidence for the eastward migration of the Alboran Sea based on regional subsidence analysis: a case for basin formation by delamination of the subcrustal lithosphere? Tectonics 14, 804–818.

Dziewonski, A.M., Woodhouse, J.H., 1983. An experiment in the systematic study of global seismicity: centroid moment-tensor solutions for 201 moderate and large earthquakes of 1981. J. Geophys. Res. 88, 3247–3271.

Faccenna, C., Piromallo, C., Crespo-Blanc, A., Jolivet, L., Rossetti, F., 2004. Lateral slab deformation and the origin of the western Mediterranean arcs. Tectonics 23, TC1012. doi:10.1029/2002TC001488.

Fadil, A., Vernant, P., McClusky, S., Reilinger, R., Gomez, F., Ben Sari, D., Mourabit, T., Feigl, K., Barazangi, M., 2006. Active tectonics of the western Mediterranean: evidence for roll-back of a delaminated subcontinental lithospheric slab beneath the Rif Mountains Morocco. Geology 34, 529–532.

Fernandes, R.M.S., Miranda, J.M., Meijninger, R.M.L., Bos, M.S., Noomen, R., Bastos, L., Ambrosius, B.A.C., Riva, R.E.M., 2007. Surface velocity field of the Ibero-Maghrebian segment of the Eurasia–Nubia plate boundary. Geophys. J. Int. 169, 315–324.

Fernández-Ibáñez, F., Soto, J.I., Zoback, M.D., Morales, J., 2007. Present-day stress field in the Gibraltar Arc (western Mediterranean). J. Geophys. Res. 112, B08404. doi:10.1029/2006JB004683.

Fukao, Y., 1973. Thrust faulting at a lithospheric plate boundary. The Portugal earthquake of 1969. Earth Planet. Sci. Lett. 18, 205–216.

Galindo- Zaldívar, J., Jabaloy, A., Serrano, I., Morales, J., González-Lodeiro, F., Torcal, F., 1999. Recent and present-day stresses in the Granada Basin (Betic Cordilleras): example of a late Miocene–present-day extensional basin in a convergent plate boundary. Tectonics 18, 686–702.

Geissler, W.H., Matias, L.M., Monna, S., Stich, D., Iben Brahim, A., Mancilla, F., Zitellini, N., NEAREST Working Group, 2009. Sub-crustal earthquakes beneath the Gulf of Cadiz — first results from seismological observations with the NEAREST OBS network. Geophy. Res. Abstr. 11 EGU2009-5641-3.

Goldstein, P., Dodge, D., Firpo, M., Minner, Lee, 2003. SAC2000: signal processing and analysis tools for seismologists and engineers. In: Lee, W.H.K., Kanamori, H., Jennings, P.C., Kisslinger, C. (Eds.), IASPEI International Handbook of Earthquake and Engineering Seismology. Academic Press, London.

Grimison, N.L., Chen, W.P., 1986. The Azores–Gibraltar plate boundary: focal mechanisms, depths of earthquakes, and their tectonic implications. J. Geophys. Res. 91, 2029–2047.

Gutscher, M.A., 2004. What caused the great Lisbon earthquake? Science 305, 1247–1248.

Gutscher, M.A., Malod, J., Rehault, J.P., Contrucci, I., Klingelhoefer, F., Mendes-Victor, L., Spakman, W., 2002. Evidence for active subduction beneath Gibraltar. Geology 30, 1071–1074.

Hanks, T.C., Kanamori, H., 1979. A moment magnitude scale. J. Geophys. Res. 84, 2348–2350.

Herrmann, R.B., Wang, C.Y., 1985. A comparison of synthetic seismograms. Bull. Seismol. Soc. Am. 75, 41–56.

Jost, M.L., Herrmann, R.B., 1989. A student's guide and review to moment tensors. Seismol. Res. Lett. 60, 37–57.

Langston, C.A., Barker, J.S., Pavlin, G.B., 1982. Point-source inversion techniques. Phys. Earth Planet. Inter. 30, 228–241.

Liu, Q., Polet, J., Komatitsch, D., Tromp, J., 2004. Spectral element moment tensor inversion for earthquakes in southern California. Bull. Seismol. Soc. Am. 94, 1748–1761.

Lonergan, L., White, N., 1997. Origin of the Betic–Rif mountain belt. Tectonics 16, 504–522.

Martínez-Díaz, J.J., 2002. Stress field variations related to fault interaction in a reverse oblique-slip fault: the Alhama de Murcia fault, Betic Cordillera, Spain. Tectonophysics 356, 291–305.

Masana, E., Martínez-Díaz, J.J., Hernández-Enrile, J.L., Santanach, P., 2004. The Alhama de Murcia fault (SE Spain), a seismogenic fault in a diffuse plate boundary: seismotectonic implications for the Ibero-Magrebian region. J. Geophys. Res. 109, B01301. doi:10.1029/2002JB002359.

McClusky, S., Reilinger, R., Mahmoud, S., Ben Sari, D., Tealeb, A., 2003. GPS constraints on Africa (Nubia) and Arabia plate motions. Geophys. J. Int. 155, 126–138.

Mezcua, J., Rueda, J., 1997. Seismological evidence for a delamination process in the lithosphere under the Alboran Sea. Geophys. J. Int. 129, 1–8.

Morales, J., Serrano, I., Jabaloy, A., Galindo-Zaldivar, J., Zhao, D., Torcal, F., Vidal, F., Gonzalez-Lodeiro, F., 1999. Active continental subduction beneath the Betic Cordillera and Alboran Sea. Geology 27, 735–738.

Platt, J.P., Vissers, R.L.M., 1989. Extensional collapse of thickened continental lithosphere: a working hypothesis for the Alboran sea and Gibraltar arc. Geology 17, 540–543.

Pondrelli, S., Morelli, A., Ekström, G., Mazza, S., Boschi, E., Dziewonski, A.M., 2002. European-Mediterranean regional centroid-moment tensors: 1997–2000. Phys. Earth Planet. Inter. 130, 71–101.

Randall, G.E., Ammon, C.J., Owens, T.J., 1995. Moment tensor estimation using regional seismograms from a Tibetan Plateau portable network deployment. Geophys. Res. Lett. 22, 1665–1668.

Rueda, J., Mézcua, J., 2005. Near-real-time seismic moment-tensor determination in Spain. Seismol. Res. Lett. 76, 455–465.

Ruiz-Constán, A., Stich, D., Galindo-Zaldívar, J., Morales, J., 2009. Is the northwestern Betic Cordillera mountain front active in the context of the convergent Eurasia-Africa plate boundary? Terra Nova 21, 352–359.

Sartori, R., Torelli, L., Zitellini, N., Peis, D., Lodolo, E., 1994. Eastern segment of the Azores–Gibraltar line (central-eastern Atlantic): an oceanic plate boundary with diffuse compressional deformation. Geology 22, 555–558.

Seber, D., Barazangi, M., Ibenbrahim, A., Demnati, A., 1996. Geophysical evidence for lithospheric delamination beneath the Alboran Sea and Rif–Betic mountains. Nature 379, 785–790.

Serpelloni, E., Vannucci, G., Pondrelli, S., Argnani, A., Casula, G., Anzidei, M., Baldi, P., Gasperini, P., 2007. Kinematics of the Western Africa–Eurasia plate boundary from focal mechanisms and GPS data. Geophys. J. Int. 169, 1180–1200.

Silver, P.G., Jordan, T.H., 1982. Optimal estimation of scalar seismic moment. Geophys. J. R. Astron. Soc. 70, 755–787.

Sipkin, S.A., 1982. Estimation of earthquake source parameters by the inversion of wave-form data: synthetic waveforms. Phys. Earth Planet. Inter. 30, 242–259.

Stich, D., Ammon, C.J., Morales, J., 2003. Moment tensor solutions for small and moderate earthquakes in the Ibero-Maghreb region. J. Geophys. Res. 108, 2148. doi:10.1029/2002JB002057.

Stich, D., Batlló, J., Macià, R., Teves-Costa, P., Morales, J., 2005a. Moment tensor inversion with single-component historical seismograms: the 1909 Benavente (Portugal) and Lambesc (France) earthquakes. Geophys. J. Int. 162, 850–858.

Stich, D., Mancilla, F., Morales, J., 2005b. Crust-mantle coupling in the Gulf of Cadiz (SW-Iberia). Geophys. Res. Lett. 32, L13306. doi:10.1029/2005GL023098.

Stich, D., Mancilla, F., Baumont, D., Morales, J., 2005c. Source analysis of the Mw 6.3 2004 Al Hoceima earthquake (Morocco) using regional apparent source time functions. J. Geophys. Res. 110, B06306. doi:10.1029/2004JB003366.

Stich, D., Serpelloni, E., Mancilla, F., Morales, J., 2006. Kinematics of the Iberia–Maghreb plate contact from seismic moment tensors and GPS observations. Tectonophysics 426, 295–317.

Stich, D., Mancilla, F., Pondrelli, S., Morales, J., 2007. Source analysis of the February 12th 2007, Mw 6.0 Horseshoe earthquake: implications for the 1755 Lisbon earthquake. Geophys. Res. Lett. 34. doi:10.1029/2007GL030012.

Tahayt, A., Mourabit, T., Rigo, A., Feigl, K.L., Fadil, A., McClusky, S., Reilinger, R., Serroukh, M., Ouazzani-Touhami, A., Ben-Sari, D., Vernant, P., 2008. Mouvements actuels des blocs tectoniques dans l'arc Bético-Rifain à partir des mesures GPS entre 1999 et 2005. C. R. Geosci. 340, 400–413.

Wessel, P., Smith, W.H.F., 1998. New, improved version of the Generic Mapping Tools released. EOS Trans. AGU 79, 579.